

CLIP-UP: CLIP-Based Unanswerable Problem Detection for Visual Question Answering

Ben Vardi¹

Oron Nir^{1,2}

Ariel Shamir¹

¹Reichman University

²Microsoft Corporation

ben.vardi01@post.runi.ac.il

niroron@microsoft.com

arik@runi.ac.il

Abstract

Recent Vision-Language Models (VLMs) have demonstrated remarkable capabilities in visual understanding and reasoning, and in particular on multiple-choice Visual Question Answering (VQA). Still, these models can make distinctly unnatural errors, for example, providing (wrong) answers to unanswerable VQA questions, such as questions asking about objects that do not appear in the image.

To address this issue, we propose CLIP-UP: CLIP-based Unanswerable Problem detection, a novel lightweight method for equipping VLMs with the ability to withhold answers to unanswerable questions. By leveraging CLIP to extract question-image alignment information, CLIP-UP requires only efficient training of a few additional layers, while keeping the original VLMs’ weights unchanged.

Tested across LLaVA models, CLIP-UP achieves state-of-the-art results on the MM-UPD benchmark for assessing unanswerability in multiple-choice VQA, while preserving the original performance on other tasks. Code and training dataset are available at <https://benvr.github.io/CLIP-UP>.

1. Introduction

A fundamental task in the domain of Vision-Language Models (VLMs) is Visual Question Answering (VQA) [4], where the model is asked a question related to a visual input. Among the various VQA formats, multiple-choice VQA stands out as particularly challenging, as it requires the model to discriminate between several plausible answer options. Recent VLMs [8, 35] excel in this task, which became a crucial benchmark for evaluating the multi-modal capabilities of VLMs.

Despite recent VLMs’ impressive advancements, a critical challenge persists: the tendency of VLMs to produce incorrect or irrelevant responses, a phenomenon commonly referred to as “hallucinations” [37, 48]. The problem is particularly concerning in VQA, where models might confidently provide answers that, while seemingly plausible, are

	Standard	Absent Answer Detection (AAD)	Incompatible Answer Set Detection (IASD)	Incompatible Visual Question Detection (IVQD)
Question	What animal is by the flowers? A. Dog B. Rabbit C. Cat	What animal is by the flowers? A. Dog B. Bird C. Cat	What animal is by the flowers? A. Sunny B. Rainy C. Snowy	What animal is by the flowers? A. Dog B. Rabbit C. Cat
LLaVA-1.5-7B	B. Rabbit ✓	C. Cat ✗	A. Sunny ✗	A. Dog ✗
LLaVA-1.5-7B + CLIP-UP	B. Rabbit ✓	Cannot answer ✓	Cannot answer ✓	Cannot answer ✓

Figure 1. CLIP-UP equips pre-trained VLMs such as LLaVA-1.5-7B [34] with the ability to detect and withhold answers to unanswerable questions, while still preserving the model’s original capabilities on standard answerable questions.

actually inconsistent with the visual content [32, 42]. This raises concerns about VLMs’ reliability and applicability, indicating the need for mitigating such hallucinations [6].

In this work, we focus on a crucial hallucination challenge within VLMs, known as the *Unsolvable Problem Detection* (UPD) challenge [42]. In this challenge, models are evaluated on their ability to detect unanswerable multiple-choice VQA questions and withhold answers when necessary. “Unanswerability” here refers to inherent issues within VQA inputs, which are usually classified into three categories [42]: (1) **Absent Answer Detection (AAD)** – detecting questions where all answer options are incorrect; (2) **Incompatible Answer Set Detection (IASD)** – detecting questions with answer options incompatible with the question; and (3) **Incompatible Visual Question Detection (IVQD)** – detecting questions where the question is incompatible with the image. See Fig. 1 for illustration.

Miyai et al. [42] demonstrated that current VLMs struggle to withhold answers for unanswerable questions. In their MM-UPD benchmark designed to test this capability, LLaVA-1.5-13B [34] for instance, never succeeds to recognize IVQD questions, providing answers even when the visual content does not make sense in connection with the question. This finding, along with others, underscores UPD as an open problem, particularly evident in open-source models [42] such as LLaVA.

An examination of LLaVA’s training data reveals a predominance of valid, answerable questions, likely contributing to its tendency to always provide an answer. While a straightforward solution involves fine-tuning or re-training the full model with data that include unanswerable questions, this approach is impractical due to the high computational and data requirements. Therefore, a pressing question arises: how can we adapt existing models to identify when they should refrain from answering in affordable costs?

To tackle this question, Miyai et al. [42] explored simple prompt engineering solutions that modify the input question to inform the model it may withhold an answer. This is done, for example, by adding a “None of the above” answer option to the options set, providing an alternative when the question is unanswerable. While appealing for its training-free nature and ease of implementation, prompt engineering was found to provide only limited improvement. More critically, these solutions modify the input based on the category of unanswerability (*e.g.*, different answer options are added for AAD and IVQD unanswerable questions), which is unknown in real-world scenarios. Another solution is to fine-tune the model on UPD-specific data [42]. Although this approach significantly enhances the model’s ability to detect unanswerable questions, its exclusive focus on UPD compromises performance on other tasks, making it an impractical solution.

To address this challenge we introduce CLIP-based Unanswerable Problem detection (CLIP-UP), a lightweight method to equip general pre-trained VLMs with the capability to detect unanswerable multiple-choice VQA questions (see Fig. 1). CLIP-UP operates by leveraging carefully crafted *correlation vectors* derived from CLIP [47] embeddings of the input image and question, encoding image-question alignment information. These vectors are projected into the VLM’s intermediate feature space, producing a new embedding vector that is seamlessly integrated into the model. CLIP-UP only trains a few linear projection layers to create this embedding vector, while leaving the original VLM weights unchanged.

Using a simple rule-based classification algorithm, we determine if the new embedding vector should be activated: for multiple-choice VQA inputs, the vector is generated and integrated to enhance UPD capabilities; otherwise, it is simply not generated, ensuring the model’s original capabilities remain intact on other tasks.

CLIP-UP’s correlation vectors are designed to capture alignment information between the input image and each answer option, as multiple-choice VQA (un)answerability relies on this alignment. CLIP [47], with its robust image-text alignment capability, is suited to provide us with this information. The effectiveness of CLIP-UP depends on the quality of the CLIP signal. In particular, we use Structure-CLIP [25], a CLIP variant that offers improved alignment

for texts with similar structures but different semantics.

Our experiments on the MM-UPD benchmark [42] show that CLIP-UP, applied across different LLaVA models [34, 35], achieves UPD performance on par with state-of-the-art full-model fine-tuning, but without its associated drawbacks. We created a new UPD dataset for training CLIP-UP, with samples across all three unanswerability categories.

Our contributions can be summarized as follows:

- We introduce CLIP-UP, a novel lightweight approach leveraging CLIP mapping to equip VLMs with UPD ability, while leaving the original VLM weights unaltered.
- We demonstrate that CLIP-UP significantly enhances UPD performance across various LLaVA models [34, 35], achieving results comparable to full-model fine-tuning and preserving performance on other tasks.
- We release our code and new UPD training dataset to support future research.

2. Related work

Vision-language models. The rapid advancements in Large Language Models (LLMs) in recent years [7, 10, 11, 55] have led to impressive performance across a wide range of text-based tasks. Building on the success of LLMs, Vision-Language Models (VLMs) have emerged by integrating visual inputs into LLMs, enabling models to reason about images and text simultaneously [1, 31, 36, 61].

VLMs typically process images through a pre-trained vision encoder, creating embeddings that are subsequently aligned with and fed into a pre-trained LLM. The pipeline is fine-tuned on paired image-text data, with different models varying in which modules are frozen or fine-tuned. For instance, LLaVA [34–36] uses a frozen CLIP [47] image encoder, and maps its embeddings to a Vicuna LLM [10] via a learnable alignment module, with the LLM being fine-tuned. BLIP-2 [31] learns a Query Transformer to extract image information from a frozen CLIP [47] or EVA-CLIP encoder [52], while keeping the LLM frozen.

Hallucination issues in VLMs. Despite their significant progress, VLMs often generate text that is semantically coherent but conflicts with the content of the input image, a problem commonly referred to as “hallucinations” [37, 48]. The causes of hallucinations are diverse, including biases in fine-tuning data [32], image encoder limitations [16, 54], and language biases from the LLM decoder [17, 43].

Given the diversity of causes, hallucination mitigation methods vary significantly. For example, Ganz et al. [16] propose making the image encoder text-aware, enabling it to focus on the text-relevant image regions. Tong et al. [54] note that CLIP image encoders struggle with certain visual patterns, and suggest the integration of self-supervised DINOv2 features [46] to alleviate related hallucinations. Ad-

ditionally, various datasets and benchmarks have been developed to study hallucinations [18, 19, 32, 53].

Although hallucination mitigation is a popular research focus, it remains a major challenge for VLMs’ applicability. In this work, we focus on a specific hallucination category, where models rarely withhold answers to unanswerable visual questions.

Unanswerable visual question answering. Visual Question Answering (VQA) [4] is a fundamental task for VLMs, where a model is shown an image and a related question and is expected to provide an accurate response. While early benchmarks focused on open-ended questions [4, 17, 29], more recent works include other VQA types, such as yes/no [14] and multiple-choice questions [30, 38, 59]. Among these, multiple-choice VQA, offering a closed set of options, has become an important VQA variant and a primary testbed for assessing VLMs, with models [1, 36, 61] rigorously tested on its benchmarks.

However, most multiple-choice VQA benchmarks contain only answerable questions, meaning that the question, image, and answers set are all compatible and a correct answer exists in the set. This setup does not reflect real-world scenarios, where questions may be unanswerable. Although some datasets consider unanswerability [20, 21], until recently none have formalized it in multiple-choice VQA.

To address this gap, Miyai et al. [42] recently introduced the Unsolvable Problem Detection (UPD) challenge, formalizing unanswerability in multiple-choice VQA. They categorized three unanswerability types (AAD, IASD, and IVQD; see explanation in Sec. 1) and published the MM-UPD benchmark, containing flawed questions alongside standard answerable questions. Unanswerability here refers to flaws inherent to the question-image pairing or the question itself, and not to knowledge gaps. Using the MM-UPD benchmark as a testbed, Miyai et al. [42] showed that VLMs often respond with an answer even when no relevant answer option exists, with open-source models like LLaVA-1.5-13B [34] showing particularly low performance.

In this work, we present a solution for the UPD challenge, leveraging CLIP in a lightweight training framework.

Efficient model editing. Model editing is a research area focused on making targeted changes to pre-trained models for specific inputs, without compromising overall performance. Efficiency is a key goal, with efforts aimed at developing methods to apply edits without high computational costs or extensive data requirements [57, 60].

Model editing has gained considerable attention in the context of LLMs, driven by the growing need to adapt models to issues such as updating outdated information and alleviating factual hallucinations [12, 22, 41]. It is also popular in text-to-image generation, where personalization may be

achieved by affordable learning of concept-specific embedding vectors [5, 15, 49, 56].

Few works have explored model editing in VLMs [2, 9, 24]. MyVLM [2], for instance, learns concept-specific embedding vectors for personalized VLM outputs. Our CLIP-UP method also introduces a new embedding vector, but to equip VLMs with the ability to withhold answers to unanswerable questions. Moreover, rather than learning the vector from scratch, we leverage CLIP’s vision-language alignment and learn a few projection layers to create it.

3. Method

3.1. Overview

CLIP-UP aims to equip pre-trained VLMs with the capability to withhold answers for unanswerable multiple-choice VQA questions, while minimizing performance degradation on standard (*i.e.*, answerable) questions, and maintaining original abilities on other tasks. Notably, CLIP-UP is not intended to enhance overall VQA performance, which would likely require extensive fine-tuning [34].

An overview of CLIP-UP applied on LLaVA [34–36] architectures is in Fig. 2a. Given an image and a multiple-choice VQA prompt, we first parse the text to separate the question and each answer option, and form individual text segments that merge the question with each answer. Each text segment is encoded by CLIP text encoder, while the image is encoded by CLIP image encoder. Each text segment encoding is multiplied element-wise by the image encoding to create *correlation vectors*. These vectors capture the alignment between the image and each answer option (see Sec. 3.2). Next, we concatenate the correlation vectors and pass them through a learnable projection layer, transforming them into a new embedding vector within the VLM’s intermediate feature space. This embedding vector is fed into the VLM alongside the standard inputs (see Sec. 3.3).

This pipeline can be used to learn a single projection for all unanswerability categories (AAD, IASD, and IVQD) together. However, a better balance across categories is achieved by first learning separate projections for each category and then learning a Mixture-of-Experts (MoE) [26] gating module that determines which “expert embedding vectors” to use, based on the input (see Sec. 3.4 and Fig. 2b).

3.2. Correlation vectors generation

The first step of CLIP-UP is generating correlation vectors. Let (T, I) be a multiple-choice VQA input, where T represents the text (both the question and answer options) and I is the image. Given such input with n options, we parse T into a pair $(Q, \{O_1, \dots, O_n\})$, where Q is the question and $\{O_1, \dots, O_n\}$ is the set of answer options. Parsing is done with a simple rule-based algorithm; see Appendix D for details.

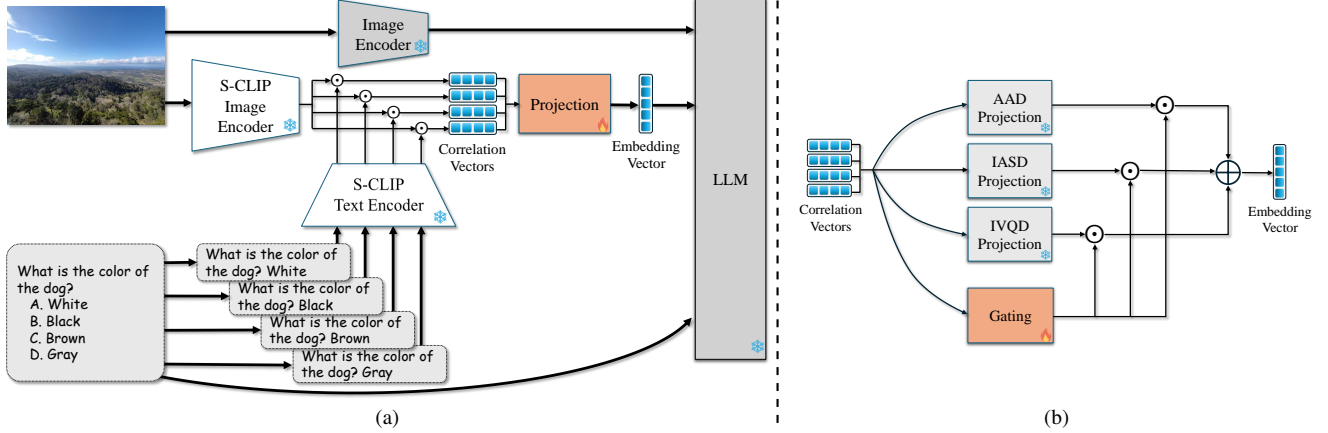


Figure 2. (a) CLIP-UP applied on LLaVA [34–36] architectures. Given an image and multiple-choice VQA prompt, the prompt is transformed into text segments merging the question with each answer option. These segments and the image are encoded by Structure-CLIP (S-CLIP) to produce embeddings, from which correlation vectors are formed via element-wise multiplication. A learnable projection module maps these vectors into LLaVA’s intermediate feature space. The resulting new embedding vector is integrated into the LLM alongside the standard inputs. (b) CLIP-UP MoE architecture. To address all unanswerability categories, a learnable gating module combines embedding vectors generated from pre-trained “expert projections” for each unanswerability category.

To contextualize each answer option O_i , we merge it with the question Q . This produces the set $\mathcal{Q}_{\text{opt}} = \{Q + O_i \mid i = 1, \dots, n\}$, where each element $s_i \in \mathcal{Q}_{\text{opt}}$ is the question followed by a single answer option. Note that using the answer options alone does not contain sufficient information, as it can lack context (e.g., “Blue” against “What color is the dress? Blue”).

We then encode each contextualized answer option $s_i \in \mathcal{Q}_{\text{opt}}$ with Structure-CLIP [25] text encoder to obtain a text embedding $\mathbf{v}_{s_i} = \text{SC}_{\text{text}}(s_i)$. The image is processed by Structure-CLIP image encoder, yielding the image embedding $\mathbf{v}_I = \text{SC}_{\text{img}}(I)$. Structure-CLIP [25] is a variant of CLIP, designed to distinguish semantically-different texts with similar structures. It is well-suited for our contextualized answer options as they share the same structure.

We generate n correlation vectors $\{\mathbf{u}_1, \dots, \mathbf{u}_n\}$ by performing element-wise multiplication between each text embedding and the image embedding:

$$\mathbf{u}_i = \mathbf{v}_I \odot \mathbf{v}_{s_i}. \quad (1)$$

Thus, rather than relying solely on scalar CLIP similarity scores (dot product of embeddings), our approach creates richer correlation vectors incorporating the similarity scores (as vectors’ sums) and additional alignment information.

Extracting these correlation vectors provides a strong prior for assessing the answerability of the VQA input. As illustrated in Fig. 3, for a standard answerable question (i.e., one having a correct answer option) paired with its correct answer, the image and text align well, leading to high CLIP similarity. Consequently, for standard questions, one correlation vector, i.e., the one corresponding to the correct answer, will exhibit high values.

Conversely, for unanswerable questions, all n correlation vectors are expected to exhibit low values, as no contextualized option aligns well with the image. This pattern occurs when all answers are relevant but incorrect (AAD), all answers are incorrect and irrelevant to the question (IASD), or the question itself is incompatible with the image (IVQD).

Therefore, due to their design, the n correlation vectors provide a strong signal for determining VQA answerability.

3.3. Learning a new projection layer

The correlation vectors capture essential alignment signal, but the VLM cannot directly interpret them, as they are neither optimized for its use nor, more critically, aligned with its feature space dimension. To address this, we concatenate the correlation vectors and project them into a vector \mathbf{e} in the VLM’s intermediate feature space, using a learnable projection layer \mathcal{P} :

$$\mathbf{e} = \mathcal{P}(\mathbf{u}), \text{ where } \mathbf{u} = [\mathbf{u}_1; \dots; \mathbf{u}_n]. \quad (2)$$

The new embedding vector \mathbf{e} , lies in the VLM’s intermediate feature space and is subsequently fed into the model.

Notably, only the projection layer is trained, while other components remain frozen, making CLIP-UP training simple and efficient. Training uses cross-entropy loss on answerable and unanswerable questions. Answerable questions have the correct option (e.g., “B”) as their ground truth text, while unanswerable questions use “I cannot answer”.

We use a simple linear layer for the projection. Since the projection input size is fixed, the concatenated correlation vectors must have fixed size as well. Given that multiple-choice questions typically have up to four options, we generate four correlation vectors for each input. For inputs with

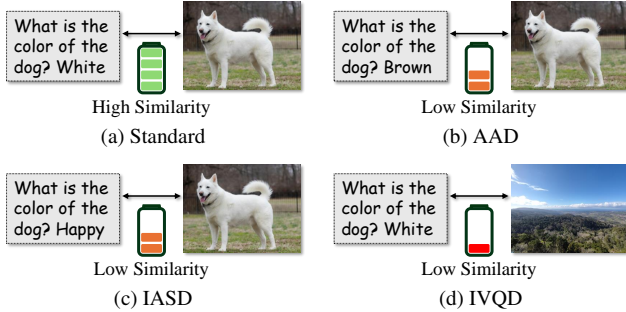


Figure 3. Our correlation vectors capture a prior for VQA answerability. (a) For a standard question, the contextualized correct answer option aligns well with the image, resulting in a correlation vector with high values. For unanswerable questions, no contextualized answer option aligns well with the image: either (b) all answer options are incorrect (AAD), (c) all answer options are incorrect and irrelevant to the question (IASD), or (d) the question is incompatible with the image (IVQD).

fewer options (three or two), we fill the remaining slots with correlation vectors generated from element-wise multiplication of the image embedding and null text embedding.

What makes CLIP-UP effective at enhancing UPD performance, even though VLMs already “see” both the image and text? We postulate that the global alignment information extracted by CLIP-UP is absent in popular VLMs [31, 34–36]. For example, although LLaVA uses a CLIP image encoder, it extracts patch features from the penultimate layer, assumed to be more effective for capturing image details [36]. In contrast, CLIP-UP equips LLaVA with global information by using CLIP’s class embedding from the last layer, explicitly trained to capture global alignment [47]. Together with the incorporation of CLIP’s text embeddings, CLIP-UP thus introduces global image-text information that LLaVA lacks.

Lastly, capturing alignment information in an embedding vector provides flexibility. During inference, a simple rule-based algorithm classifies inputs, allowing us to generate and use the vector only for multiple-choice VQA inputs, ensuring that performance on other tasks remains unaffected.

3.4. Learning mixture of experts

We aim to equip VLMs with the ability to handle all unanswerability categories together, a more realistic scenario than focusing only on a single one (*e.g.*, only AAD). While the method described so far can learn a single projection to handle all categories, we find that a Mixture of Experts (MoE) [26] approach is more effective. In this approach, we first learn separate “expert projections” for each category (AAD, IASD, and IVQD), specializing in each challenge individually. We then train a MoE gating module that combines the embedding vectors produced from each expert projection based on the input. See Fig. 2b for illustration.

The gating module is a simple classifier comprising a linear layer followed by a softmax operation. It takes the correlation vectors concatenation \mathbf{u} from a multiple-choice VQA input and classifies it into six classes: AAD, IASD, IVQD, and their corresponding answerable standard types. We use six classes instead of the more immediate choice of four (one for each challenge and one for standard questions) for two reasons: first, it is unclear which expert to assign to the “standard” class; second, answerable questions also vary in nature, a distinction likely reflected in the correlation vectors. This is due to the training data being organized into pairs of standard questions and corresponding unanswerable variants (see Sec. 4.1). Thus, for instance, a standard question paired with an AAD question must have exactly one correct option, with all others clearly incorrect.

Based on the classification scores for the six classes, we set the new embedding vector \mathbf{e} as a weighted average of three “expert projected embedding vectors”:

$$\mathbf{e} = \sum_c w_c \mathcal{P}_c(\mathbf{u}), \quad c \in \{\text{AAD, IASD, IVQD}\} \quad (3)$$

where $\mathcal{P}_c(\mathbf{u})$ represents the expert projection for unanswerability category c , and w_c is a scalar representing the summed classification scores of both standard and unanswerable questions within class c , and $\sum_c w_c = 1$.

Our MoE approach uses four projection layers: three for the expert projections and one for the gating. Training the gating module is fast, as it only involves classifying correlation vector inputs, without requiring text generation.

Note that we do not expect the gating classifier to be highly accurate. If it were, it would have solved the UPD challenge on its own. Instead, we expect it to perform reasonably well, with the expert projections compensating for its limitations. Since challenges are distinct but related (*e.g.*, IASD may be seen as an extreme case of AAD, where answer options are irrelevant to the question), even a moderately accurate gating can achieve a balanced performance across the categories. Lastly, since the gating module is model-independent, it can be reused across different VLMs.

4. Experiments

We primarily assess CLIP-UP’s ability to withhold answers for unanswerable questions while minimizing degradation on answerable ones. CLIP-UP is designed to preserve original performance on tasks beyond multiple-choice VQA, a property we also validate. For clarity, “CLIP-UP” here refers to our MoE architecture.

4.1. Dataset

We created a dataset for training CLIP-UP, containing answerable and unanswerable questions across AAD, IASD, and IVQD. The dataset is organized into question pairs,

Method	AAD			IASD			IVQD			Dual Avg.
	Stand.	UPD	Dual	Stand.	UPD	Dual	Stand.	UPD	Dual	
Original Model	70.73	0.00	0.00	68.12	0.33	0.33	65.45	0.00	0.00	0.11
Base Setting	69.15	1.46	1.46	66.81	19.48	12.73	63.76	0.28	0.28	4.82
Additional-Option*	68.29	48.66	40.85	65.61	78.02	51.03	64.33	27.81	22.19	38.02
Additional-Instruction*	69.02	33.90	28.05	66.16	65.72	43.74	64.61	32.02	24.44	32.08
CLIP-UP-Experts*	62.44	90.73	58.41	62.68	88.14	55.71	62.92	87.64	55.34	56.49
Fine-tuning [†]	64.63	56.34	43.78	61.92	87.81	54.73	61.24	85.96	52.25	50.25
CLIP-UP (ours)	59.39	77.07	48.54	57.45	89.12	52.34	57.58	88.20	53.09	51.32

(a) LLaVA-1.5-7B

Method	AAD			IASD			IVQD			Dual Avg.
	Stand.	UPD	Dual	Stand.	UPD	Dual	Stand.	UPD	Dual	
Original Model	76.71	0.00	0.00	73.23	0.11	0.00	71.35	0.00	0.00	0.00
Base Setting	72.32	23.78	17.80	69.75	49.62	31.66	68.82	44.66	33.15	27.54
Additional-Option*	75.85	18.41	18.05	72.47	39.28	29.92	70.79	46.35	38.20	28.72
Additional-Instruction*	67.07	48.66	38.29	63.87	87.81	57.02	68.82	71.91	54.49	49.93
CLIP-UP-Experts*	70.37	81.22	60.24	64.09	93.14	59.96	67.42	93.82	65.17	61.79
Chain-of-Thought	60.00	60.50	42.80	56.40	70.80	43.90	59.00	75.30	47.50	44.73
Self-Reflection	66.20	50.00	37.80	62.60	55.80	36.70	59.80	61.50	39.00	37.83
Fine-tuning [†]	69.15	58.54	47.56	65.51	91.19	59.85	67.42	86.24	59.55	55.65
CLIP-UP (ours)	68.17	69.76	52.56	64.20	84.33	55.39	60.67	89.04	56.18	54.71

(b) LLaVA-NeXT-13B

Table 1. CLIP-UP results (%) on the MM-UPD benchmark [42] for (a) LLaVA-1.5-7B and (b) LLaVA-NeXT-13B. Metrics include standard, UPD, dual, and average dual accuracies, all based on circular evaluation. The best-performing methods that do not assume unavailable knowledge of unanswerability categories are bolded. *Methods assuming knowledge of unanswerability categories. [†]Fine-tuning degrades performance on other tasks, making it an impractical solution.

with each pair consisting of a standard question and its corresponding unanswerable variant. For instance, an AAD unanswerable question is generated by removing the correct option from a standard question.

The dataset includes 293, 189, and 307 question pairs for AAD, IASD, and IVQD, respectively. For each category, 30 question pairs are allocated to the validation set, with the rest in the training set. The dataset is available on our project page. Further details are provided in Appendix C.

4.2. Training

We evaluate CLIP-UP on two models: LLaVA-1.5-7B [34] and LLaVA-NeXT-13B [35]. All projections are trained for 3 epochs on data from our dataset, with each expert projection trained only on its challenge data (e.g., only AAD data), and the gating module trained on data from all challenges. We use an effective batch size of 8 for both models. Each batch contains 4 pairs of corresponding answerable and unanswerable questions, which we find to enhance training stability. See Appendix A further technical details.

We generate the correlation vectors using Structure-CLIP [25]. As Structure-CLIP’s weights are unavailable, we fine-tune CLIP ViT-L/14@336 [47] to replicate it.

4.3. Comparisons

We first compare CLIP-UP to the original LLaVA models, where multiple-choice VQA is evaluated with the instruction “Answer directly with the letter of the correct option from the given choices” appended to the prompt [34].

We also compare CLIP-UP to three prompt engineering settings from [42]: (1) Base Prompt Setting: uses only the multiple-choice VQA prompt without additional instructions. As this setting does not explicitly encourage choosing an answer, it identifies unanswerable questions better than the original setup; (2) Additional-Option Setting: adds an option depending on the unanswerability category (“None of the above” for AAD and IASD, or “The image and question are irrelevant” for IVQD), and includes the original instruction. This setting ensures that a correct answer is always present and encourages the model to select one; (3) Additional-Instruction Setting: adds an instruction to encourage withholding an answer when appropriate. The instructions vary by the unanswerability category and are similar to the extra option in the Additional-Option Setting.

Note that settings (2) and (3) assume knowledge of the input’s unanswerability category, which is not the case in real-world scenarios. They are thus meant to test mod-

els’ capabilities via prompt engineering rather than serve as practical solutions.

Additionally, we compare CLIP-UP to full-model Low-Rank Adaptation (LoRA) [23] fine-tuning, as done in [42].

Finally, we compare to two prompt engineering methods proposed in [3]. The first employs zero-shot Chain-of-Thought [28] reasoning by appending the phrase “Let’s think step by step” to the multiple-choice VQA prompt, encouraging the model to reason more carefully. The second uses self-reflection [27] by prompting the model to evaluate its own response. The results for these methods are taken directly from [3] and reported only for LLaVA-NeXT-13B.

4.4. Benchmarks and evaluation metrics

UPD experiments. Our main experiments evaluate CLIP-UP on the MM-UPD benchmark [42], which consists of three sub-benchmarks for AAD, IASD, and IVQD. Each sub-benchmark contains pairs of multiple-choice VQA questions, an answerable one and an unanswerable one. To account for options order variation, questions are repeated up to n times (where n is the number of options), with a different circular shift applied to the options each time.

Evaluation on the MM-UPD benchmark involves five metrics: regular standard accuracy, regular UPD accuracy, circular standard accuracy, circular UPD accuracy, and circular dual accuracy. Regular standard and UPD accuracies measure the percentage of correct answers to individual questions, for standard answerable questions and unanswerable questions, respectively. Circular standard and UPD accuracies follow the CircularEval evaluation strategy [38], assessing accuracy across all circular shifts of options by counting success only if all shifts are answered correctly.

Circular dual accuracy [42] requires to correctly answer all circular variants of both standard questions and their unanswerable pairs. High dual accuracy thus indicates consistent discernment of answerability. We use dual accuracy as our main metric, along with circular standard and UPD accuracies. To measure accuracies, we extract the selected option from the VLM’s prediction as done in [42].

Experiments on other tasks. We demonstrate that CLIP-UP maintains performance on tasks beyond multiple-choice VQA, including yes/no questions (MME [14]), open-ended questions (MM-VET [58]), and instruction-following abilities (LLaVA-Bench In-the-Wild [36]).

4.5. Results

UPD results. The UPD results of CLIP-UP on LLaVA-1.5-7B and LLaVA-NeXT-13B are presented in Tab. 1. Our primary metric is the average dual accuracy, namely the dual accuracy average across all unanswerability categories.

CLIP-UP demonstrates strong performance across both tested models, achieving comparable average dual accu-

	MME			MM -VET	LLaVA -Bench
	Score	Acc.	Y/N		
Fine-tuning	1626.3	69.4	96.6	31.7	54.5
CLIP-UP	1671.4	75.5	99.2	33.3	60.6

Table 2. Results on tasks beyond multiple-choice VQA on LLaVA-1.5-7B. CLIP-UP matches original performance, thus we omit a row for the original model. For all metrics higher values indicate better performance. See Appendix B for details.

racy with state-of-the-art full-model fine-tuning (+1.07% on LLaVA-1.5-7B and -0.94% on LLaVA-NeXT-13B).

However, since full-model fine-tuning is optimized exclusively for multiple-choice VQA, it degrades performance on other tasks, making it an impractical solution for equipping models with UPD capability (see below where we validate this). In contrast, CLIP-UP preserves the original model’s performance on other tasks. CLIP-UP also offers other advantages: LoRA fine-tuning demands at least x9 more storage space than CLIP-UP and over than x5 data.

We also present CLIP-UP results assuming the knowledge of the unanswerability category is available. These results correspond to non-MoE CLIP-UPs, each with a single projection trained for one unanswerability category (denoted as CLIP-UP-Experts in Tab. 1). While impractical for real-world scenarios, these results show notably better performance, underscoring CLIP-UP’s potential with more precise gating.

While CLIP-UP improves UPD performance, its lightweight training is not intended to boost standard accuracy. Consequently, the original model’s standard accuracy serves as an upper bound for dual accuracy. Thus, CLIP-UP is closer to its upper limit than it may seem. For example, on LLaVA-1.5-7B it achieves 51.32% average dual accuracy, where the upper bound is 68.1% (the original model average standard accuracy).

Results on other tasks. We now address the real-world case where inputs are not always multiple-choice VQA questions. As noted in Sec. 3.3, we use a simple rule-based algorithm to determine whether an input is a multiple-choice VQA question.

We find that this simple algorithm is highly effective on all non-multiple-choice VQA tasks tested, identifying 100% of the inputs as non multiple-choice VQA inputs. Consequently, since CLIP-UP does not alter the original VLM weights, it maintains the original VLM’s performance on non-multiple-choice tasks.

Tab. 2 compares CLIP-UP and full-model fine-tuning on LLaVA-1.5-7B. Fine-tuning shows expected performance degradation across all tasks. For example, on MME [14], the fine-tuned model provides irrelevant responses more of-

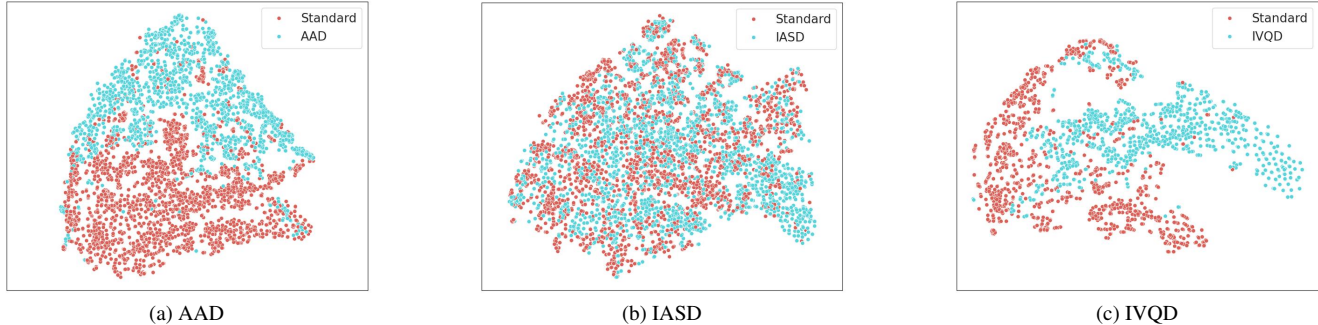


Figure 4. t-SNE plots of embedding vectors generated by CLIP-UP on LLaVA-NeXT-13B, for all samples in the MM-UPD benchmark [42].

	AAD			IASD			IVQD			Dual
	Stand.	UPD	Dual	Stand.	UPD	Dual	Stand.	UPD	Dual	Avg.
CLIP-UP-AAD	62.44	90.73	58.41	59.30	69.86	42.55	53.09	62.92	33.71	44.89
CLIP-UP-IASD	65.12	45.00	35.37	62.68	88.14	55.71	60.39	54.21	36.80	42.63
CLIP-UP-IVQD	64.15	29.88	20.73	62.46	66.70	42.33	62.92	87.64	55.34	39.47
Learning Emb. from Scratch	60.00	16.22	13.41	56.15	45.48	23.61	53.93	36.80	19.10	18.71
CLIP-UP from Similarities	68.41	11.83	10.00	66.16	42.44	27.20	65.17	39.89	26.12	21.11
CLIP-UP without S-CLIP	58.66	64.02	40.37	56.04	94.02	52.23	57.30	62.64	39.89	44.16
CLIP-UP without MoE	63.66	61.71	44.15	61.15	87.70	54.08	60.11	81.46	51.12	49.78
CLIP-UP (ours)	59.39	77.07	48.54	57.45	89.12	52.34	57.58	88.20	53.09	51.32

Table 3. CLIP-UP ablation studies results (%) on LLaVA-1.5-7B.

ten (instead of “yes” or “no”). On LLaVA-Bench [36], the model incorrectly replies “I cannot answer” for 8.3% of inputs (not shown in Tab. 2), underscoring its limitations.

4.6. Analysis and ablation studies

Fig. 4 visualizes the projections learned by CLIP-UP with t-SNE plots of embedding vectors generated from all samples in the three MM-UPD sub-benchmarks. As CLIP-UP is intended to discern answerable questions from unanswerable ones, we expect t-SNE to reveal distinct clusters for these two groups. And indeed, the visualization shows clear clustering for AAD and IVQD, suggesting the projection captures meaningful information. However, IASD clustering is less distinct. We assume this is because the correlation vectors are less suited to capture IASD’s textual inconsistency issues (*i.e.*, question-option inconsistencies).

We also conduct ablation studies to assess the impact of CLIP-UP’s components, with results for LLaVA-1.5-7B in Tab. 3. First, we evaluate each specialized expert CLIP-UP model (CLIP-UP-AAD/IASD/IVQD) on all challenges (lines 1-3 in Tab. 3). As expected, each model performs best on the challenge it was trained on, but also shows gains on others, suggesting that the unanswerability categories are interrelated. Specifically, training on AAD or IVQD data yields reasonable results for IASD, a point also noted in [42]. We postulate it is since IASD is related to both

AAD and IVQD. For instance, IASD is similar to IVQD since its answer options are likely irrelevant to the image.

We examine the impact of using CLIP by trying to learn an embedding vector from scratch (line 4). This approach is inferior to using CLIP, confirming that CLIP is a key factor in CLIP-UP. We also test a CLIP-UP variant where the projection is based on four scalar CLIP similarities rather than on four correlation vectors (line 5). This alternative yields weaker results, underscoring the value of the richer information within the correlation vectors.

Next, we test CLIP-UP using CLIP ViT-L/14@336px for generating the correlation vectors, instead of Structure-CLIP (line 6). While standard CLIP achieves reasonable results, they are markedly lower than those of our full CLIP-UP, underscoring Structure-CLIP’s importance. Finally, we test CLIP-UP trained on data from all challenges without MoE (line 7). This setup performs well, but incorporating MoE provides a 1.54% boost in average dual accuracy.

5. Conclusion and future directions

This paper introduces CLIP-UP, a lightweight method for equipping pre-trained VLMs with the capability to withhold responses to unanswerable multiple-choice VQA questions. CLIP-UP leverages CLIP to learn only a few linear projections to achieve this capability, without altering the original VLM weights. Demonstrated on LLaVA models, CLIP-UP

achieves performance on par with full-model fine-tuning while not degrading performance on other tasks.

Although CLIP-UP achieves strong results, there is room for improvement. One direction is to enrich the correlation vector with signals beyond image-text alignment. This may be especially effective for IASD, which involves intra-text inconsistencies that the current correlation vector may not fully capture. Another direction is to improve the current (naive) gating mechanism, which has the potential to boost average dual accuracy by over than 5% (see Tab. 1).

References

- [1] Josh Achiam, Steven Adler, Sandhini Agarwal, Lama Ahmad, Ilge Akkaya, Florencia Leoni Aleman, Diogo Almeida, Janko Altenschmidt, Sam Altman, Shyamal Anadkat, et al. GPT-4 technical report. *arXiv preprint arXiv:2303.08774*, 2023. 2, 3
- [2] Yuval Alaluf, Elad Richardson, Sergey Tulyakov, Kfir Aberman, and Daniel Cohen-Or. MyVLM: Personalizing VLMs for user-specific queries. In *European Conference on Computer Vision*, pages 73–91. Springer, 2025. 3
- [3] Anonymous. Unsolvable problem detection: Evaluating trustworthiness of large multimodal models, 2024. Manuscript submitted to ICLR; available on OpenReview. 7
- [4] Stanislaw Antol, Aishwarya Agrawal, Jiasen Lu, Margaret Mitchell, Dhruv Batra, C Lawrence Zitnick, and Devi Parikh. VQA: Visual question answering. In *Proceedings of the IEEE international conference on computer vision*, pages 2425–2433, 2015. 1, 3
- [5] Omri Avrahami, Kfir Aberman, Ohad Fried, Daniel Cohen-Or, and Dani Lischinski. Break-A-Scene: Extracting multiple concepts from a single image. In *SIGGRAPH Asia 2023 Conference Papers*, pages 1–12, 2023. 3
- [6] Zechen Bai, Pichao Wang, Tianjun Xiao, Tong He, Zongbo Han, Zheng Zhang, and Mike Zheng Shou. Hallucination of multimodal large language models: A survey. *arXiv preprint arXiv:2404.18930*, 2024. 1
- [7] Tom B. Brown, Benjamin Mann, Nick Ryder, Melanie Subbiah, Jared Kaplan, Prafulla Dhariwal, Arvind Neelakantan, Pranav Shyam, Girish Sastry, Amanda Askell, et al. Language models are few-shot learners. *arXiv preprint arXiv:2005.14165*, 2020. 2
- [8] Jun Chen, Deyao Zhu, Xiaoqian Shen, Xiang Li, Zechu Liu, Pengchuan Zhang, Raghuraman Krishnamoorthi, Vikas Chandra, Yunyang Xiong, and Mohamed Elhoseiny. MiniGPT-v2: large language model as a unified interface for vision-language multi-task learning. *arXiv preprint arXiv:2310.09478*, 2023. 1
- [9] Siyuan Cheng, Bozhong Tian, Qingbin Liu, Xi Chen, Yongheng Wang, Huajun Chen, and Ningyu Zhang. Can we edit multimodal large language models? *arXiv preprint arXiv:2310.08475*, 2023. 3
- [10] Wei-Lin Chiang, Zhuohan Li, Zi Lin, Ying Sheng, Zhanghao Wu, Hao Zhang, Lianmin Zheng, Siyuan Zhuang, Yonghao Zhuang, Joseph E Gonzalez, et al. Vicuna: An open-source chatbot impressing gpt-4 with 90%* chatgpt quality. *See https://vicuna.lmsys.org (accessed 14 April 2023)*, 2(3):6, 2023. 2
- [11] Aakanksha Chowdhery, Sharan Narang, Jacob Devlin, Maarten Bosma, Gaurav Mishra, Adam Roberts, Paul Barham, Hyung Won Chung, Charles Sutton, Sebastian Gehrmann, et al. PaLM: Scaling language modeling with pathways. *Journal of Machine Learning Research*, 24(240): 1–113, 2023. 2
- [12] Nicola De Cao, Wilker Aziz, and Ivan Titov. Editing factual knowledge in language models. *arXiv preprint arXiv:2104.08164*, 2021. 3
- [13] Haodong Duan, Junming Yang, Yuxuan Qiao, Xinyu Fang, Lin Chen, Yuan Liu, Xiaoyi Dong, Yuhang Zang, Pan Zhang, Jiaqi Wang, et al. VLMEvalKit: An open-source toolkit for evaluating large multi-modality models. In *Proceedings of the 32nd ACM International Conference on Multimedia*, pages 11198–11201, 2024. 1
- [14] Chaoyou Fu, Peixian Chen, Yunhang Shen, Yulei Qin, Mengdan Zhang, Xu Lin, Jinrui Yang, Xiawu Zheng, Ke Li, Xing Sun, et al. MME: A comprehensive evaluation benchmark for multimodal large language models. *arXiv preprint arXiv:2306.13394*, 2023. 3, 7, 2
- [15] Rinon Gal, Yuval Alaluf, Yuval Atzmon, Or Patashnik, Amit H Bermano, Gal Chechik, and Daniel Cohen-Or. An image is worth one word: Personalizing text-to-image generation using textual inversion. *arXiv preprint arXiv:2208.01618*, 2022. 3
- [16] Roy Ganz, Yair Kittenplon, Aviad Aberdam, Elad Ben Avraham, Oren Nuriel, Shai Mazor, and Ron Litman. Question aware vision transformer for multimodal reasoning. In *Proceedings of the IEEE/CVF Conference on Computer Vision and Pattern Recognition*, pages 13861–13871, 2024. 2
- [17] Yash Goyal, Tejas Khot, Douglas Summers-Stay, Dhruv Batra, and Devi Parikh. Making the V in VQA matter: Elevating the role of image understanding in visual question answering. In *Proceedings of the IEEE conference on computer vision and pattern recognition*, pages 6904–6913, 2017. 2, 3
- [18] Tianrui Guan, Fuxiao Liu, Xiyang Wu, Ruiqi Xian, Zongxia Li, Xiaoyu Liu, Xijun Wang, Lichang Chen, Furong Huang, Yaser Yacoob, et al. HALLUSIONBENCH: an advanced diagnostic suite for entangled language hallucination and visual illusion in large vision-language models. In *Proceedings of the IEEE/CVF Conference on Computer Vision and Pattern Recognition*, pages 14375–14385, 2024. 3
- [19] Anisha Gunjal, Jihan Yin, and Erhan Bas. Detecting and preventing hallucinations in large vision language models. In *Proceedings of the AAAI Conference on Artificial Intelligence*, pages 18135–18143, 2024. 3
- [20] Yangyang Guo, Fangkai Jiao, Zhiqi Shen, Liqiang Nie, and Mohan Kankanhalli. UNK-VQA: A dataset and a probe into the abstention ability of multi-modal large models. *IEEE Transactions on Pattern Analysis and Machine Intelligence*, 2024. 3
- [21] Danna Gurari, Qing Li, Abigale J Stangl, Anhong Guo, Chi Lin, Kristen Grauman, Jiebo Luo, and Jeffrey P Bigham. VizWiz grand challenge: Answering visual questions from

- blind people. In *Proceedings of the IEEE conference on computer vision and pattern recognition*, pages 3608–3617, 2018. 3
- [22] Thomas Hartvigsen, Swami Sankaranarayanan, Hamid Palangi, Yoon Kim, and Marzyeh Ghassemi. Aging with GRACE: Lifelong model editing with discrete key-value adaptors. In *Advances in Neural Information Processing Systems*, 2023. 3
- [23] Edward J Hu, Yelong Shen, Phillip Wallis, Zeyuan Allen-Zhu, Yuanzhi Li, Shean Wang, Lu Wang, and Weizhu Chen. LoRA: Low-rank adaptation of large language models. *arXiv preprint arXiv:2106.09685*, 2021. 7, 1
- [24] Han Huang, Haitian Zhong, Tao Yu, Qiang Liu, Shu Wu, Liang Wang, and Tieniu Tan. VLKEB: A large vision-language model knowledge editing benchmark, 2024. 3
- [25] Yufeng Huang, Jiji Tang, Zhuo Chen, Rongsheng Zhang, Xinfeng Zhang, Weijie Chen, Zeng Zhao, Tangjie Lv, Zhipeng Hu, and Wen Zhang. Structure-CLIP: Enhance multi-modal language representations with structure knowledge. *arXiv preprint arXiv:2305.06152*, 2(3), 2023. 2, 4, 6, 1
- [26] Robert A Jacobs, Michael I Jordan, Steven J Nowlan, and Geoffrey E Hinton. Adaptive mixtures of local experts. *Neural computation*, 3(1):79–87, 1991. 3, 5
- [27] Saurav Kadavath, Tom Conerly, Amanda Askell, Tom Henighan, Dawn Drain, Ethan Perez, Nicholas Schiefer, Zac Hatfield-Dodds, Nova DasSarma, Eli Tran-Johnson, et al. Language models (mostly) know what they know. *arXiv preprint arXiv:2207.05221*, 2022. 7
- [28] Takeshi Kojima, Shixiang Shane Gu, Machel Reid, Yutaka Matsuo, and Yusuke Iwasawa. Large language models are zero-shot reasoners. *Advances in neural information processing systems*, 35:22199–22213, 2022. 7
- [29] Ranjay Krishna, Yuke Zhu, Oliver Groth, Justin Johnson, Kenji Hata, Joshua Kravitz, Stephanie Chen, Yannis Kalantidis, Li-Jia Li, David A Shamma, et al. Visual genome: Connecting language and vision using crowdsourced dense image annotations. *International journal of computer vision*, 123:32–73, 2017. 3
- [30] Bohao Li, Rui Wang, Guangzhi Wang, Yuying Ge, Yixiao Ge, and Ying Shan. SEED-Bench: Benchmarking multi-modal LLMs with generative comprehension. *arXiv preprint arXiv:2307.16125*, 2023. 3
- [31] Junnan Li, Dongxu Li, Silvio Savarese, and Steven Hoi. BLIP-2: Bootstrapping language-image pre-training with frozen image encoders and large language models. In *International conference on machine learning*, pages 19730–19742. PMLR, 2023. 2, 5
- [32] Yifan Li, Yifan Du, Kun Zhou, Jinpeng Wang, Wayne Xin Zhao, and Ji-Rong Wen. Evaluating object hallucination in large vision-language models. *arXiv preprint arXiv:2305.10355*, 2023. 1, 2, 3
- [33] Tsung-Yi Lin, Michael Maire, Serge Belongie, James Hays, Pietro Perona, Deva Ramanan, Piotr Dollár, and C Lawrence Zitnick. Microsoft COCO: Common objects in context. In *Computer Vision–ECCV 2014: 13th European Conference, Zurich, Switzerland, September 6–12, 2014, Proceedings, Part V 13*, pages 740–755. Springer, 2014. 1, 2, 3
- [34] Haotian Liu, Chunyuan Li, Yuheng Li, and Yong Jae Lee. Improved baselines with visual instruction tuning. In *Proceedings of the IEEE/CVF Conference on Computer Vision and Pattern Recognition*, pages 26296–26306, 2024. 1, 2, 3, 4, 5, 6
- [35] Haotian Liu, Chunyuan Li, Yuheng Li, Bo Li, Yuanhan Zhang, Sheng Shen, and Yong Jae Lee. LLaVA-NeXT: Improved reasoning, ocr, and world knowledge, 2024. 1, 2, 6
- [36] Haotian Liu, Chunyuan Li, Qingyang Wu, and Yong Jae Lee. Visual instruction tuning. *Advances in neural information processing systems*, 36, 2024. 2, 3, 4, 5, 7, 8, 1
- [37] Hanchao Liu, Wenyuan Xue, Yifei Chen, Dapeng Chen, Xiutian Zhao, Ke Wang, Liping Hou, Rongjun Li, and Wei Peng. A survey on hallucination in large vision-language models. *arXiv preprint arXiv:2402.00253*, 2024. 1, 2
- [38] Yuan Liu, Haodong Duan, Yuanhan Zhang, Bo Li, Songyang Zhang, Wangbo Zhao, Yike Yuan, Jiaqi Wang, Conghui He, Ziwei Liu, et al. MMBench: Is your multi-modal model an all-around player? In *European Conference on Computer Vision*, pages 216–233. Springer, 2024. 3, 7, 2
- [39] Ilya Loshchilov and Frank Hutter. SGDR: Stochastic gradient descent with warm restarts. In *International Conference on Learning Representations*, 2017. 1
- [40] Ilya Loshchilov and Frank Hutter. Decoupled weight decay regularization. In *International Conference on Learning Representations*, 2019. 1
- [41] Eric Mitchell, Charles Lin, Antoine Bosselut, Chelsea Finn, and Christopher D Manning. Fast model editing at scale. *arXiv preprint arXiv:2110.11309*, 2021. 3
- [42] Atsuyuki Miyai, Jingkan Yang, Jingyang Zhang, Yifei Ming, Qing Yu, Go Irie, Yixuan Li, Hai Li, Ziwei Liu, and Kiyoharu Aizawa. Unsolvable problem detection: Evaluating trustworthiness of vision language models. *arXiv preprint arXiv:2403.20331*, 2024. 1, 2, 3, 6, 7, 8, 4
- [43] Yulei Niu, Kaihua Tang, Hanwang Zhang, Zhiwu Lu, Xian-Sheng Hua, and Ji-Rong Wen. Counterfactual VQA: A cause-effect look at language bias. In *Proceedings of the IEEE/CVF conference on computer vision and pattern recognition*, pages 12700–12710, 2021. 2
- [44] OpenAI. GPT-3.5-turbo-0125, 2023. 1
- [45] OpenAI. GPT-4o mini, 2024. 2, 3
- [46] Maxime Oquab, Timothée Darcet, Théo Moutakanni, Huy Vo, Marc Szafraniec, Vasil Khalidov, Pierre Fernandez, Daniel Haziza, Francisco Massa, Alaaeldin El-Nouby, et al. DINOv2: Learning robust visual features without supervision. *arXiv preprint arXiv:2304.07193*, 2023. 2
- [47] Alec Radford, Jong Wook Kim, Chris Hallacy, Aditya Ramesh, Gabriel Goh, Sandhini Agarwal, Girish Sastry, Amanda Askell, Pamela Mishkin, Jack Clark, et al. Learning transferable visual models from natural language supervision. In *International conference on machine learning*, pages 8748–8763. PMLR, 2021. 2, 5, 6, 1
- [48] Anna Rohrbach, Lisa Anne Hendricks, Kaylee Burns, Trevor Darrell, and Kate Saenko. Object hallucination in image captioning. *arXiv preprint arXiv:1809.02156*, 2018. 1, 2
- [49] Nataniel Ruiz, Yuanzhen Li, Varun Jampani, Yael Pritch, Michael Rubinstein, and Kfir Aberman. DreamBooth: Fine

- tuning text-to-image diffusion models for subject-driven generation. In *Proceedings of the IEEE/CVF conference on computer vision and pattern recognition*, pages 22500–22510, 2023. 3
- [50] Dustin Schwenk, Apoorv Khandelwal, Christopher Clark, Kenneth Marino, and Roozbeh Mottaghi. A-OKVQA: A benchmark for visual question answering using world knowledge. In *European conference on computer vision*, pages 146–162. Springer, 2022. 2
- [51] Oleksii Sidorov, Ronghang Hu, Marcus Rohrbach, and Amanpreet Singh. TextCaps: a dataset for image captioning with reading comprehension. In *Computer Vision—ECCV 2020: 16th European Conference, Glasgow, UK, August 23–28, 2020, Proceedings, Part II 16*, pages 742–758. Springer, 2020. 2, 3
- [52] Quan Sun, Yuxin Fang, Ledell Wu, Xinlong Wang, and Yue Cao. EVA-CLIP: Improved training techniques for CLIP at scale. *arXiv preprint arXiv:2303.15389*, 2023. 2
- [53] Zhiqing Sun, Sheng Shen, Shengcao Cao, Haotian Liu, Chunyuan Li, Yikang Shen, Chuang Gan, Liang-Yan Gui, Yu-Xiong Wang, Yiming Yang, et al. Aligning large multimodal models with factually augmented RHLF. *arXiv preprint arXiv:2309.14525*, 2023. 3
- [54] Shengbang Tong, Zhuang Liu, Yuexiang Zhai, Yi Ma, Yann LeCun, and Saining Xie. Eyes wide shut? exploring the visual shortcomings of multimodal llms. In *Proceedings of the IEEE/CVF Conference on Computer Vision and Pattern Recognition*, pages 9568–9578, 2024. 2
- [55] Hugo Touvron, Thibaut Lavril, Gautier Izacard, Xavier Martinet, Marie-Anne Lachaux, Timothée Lacroix, Baptiste Rozière, Naman Goyal, Eric Hambro, Faisal Azhar, et al. LLaMA: Open and efficient foundation language models. *arXiv preprint arXiv:2302.13971*, 2023. 2
- [56] Yael Vinker, Andrey Voynov, Daniel Cohen-Or, and Ariel Shamir. Concept decomposition for visual exploration and inspiration. *ACM Transactions on Graphics (TOG)*, 42(6): 1–13, 2023. 3
- [57] Yunzhi Yao, Peng Wang, Bozhong Tian, Siyuan Cheng, Zhoubo Li, Shumin Deng, Huajun Chen, and Ningyu Zhang. Editing large language models: Problems, methods, and opportunities. *arXiv preprint arXiv:2305.13172*, 2023. 3
- [58] Weihao Yu, Zhengyuan Yang, Linjie Li, Jianfeng Wang, Kevin Lin, Zicheng Liu, Xinchao Wang, and Lijuan Wang. MM-Vet: Evaluating large multimodal models for integrated capabilities. *arXiv preprint arXiv:2308.02490*, 2023. 7, 2
- [59] Xiang Yue, Yuansheng Ni, Kai Zhang, Tianyu Zheng, Ruoqi Liu, Ge Zhang, Samuel Stevens, Dongfu Jiang, Weiming Ren, Yuxuan Sun, et al. MMMU: A massive multi-discipline multimodal understanding and reasoning benchmark for expert AGI. In *Proceedings of the IEEE/CVF Conference on Computer Vision and Pattern Recognition*, pages 9556–9567, 2024. 3
- [60] Ningyu Zhang, Yunzhi Yao, Bozhong Tian, Peng Wang, Shumin Deng, Mengru Wang, Zekun Xi, Shengyu Mao, Jintian Zhang, Yuansheng Ni, et al. A comprehensive study of knowledge editing for large language models. *arXiv preprint arXiv:2401.01286*, 2024. 3
- [61] Deyao Zhu, Jun Chen, Xiaoqian Shen, Xiang Li, and Mohamed Elhoseiny. MiniGPT-4: Enhancing vision-language understanding with advanced large language models. *arXiv preprint arXiv:2304.10592*, 2023. 2, 3

CLIP-UP: CLIP-Based Unanswerable Problem Detection for Visual Question Answering

Supplementary Material

A. Implementation details

CLIP-UP. CLIP-UP involves two training settings: one for the expert projections (described in Sec. 3.3), and another for the MoE gating module (described in Sec. 3.4).

In both settings, we use the AdamW optimizer [40] with weight decay of 0.0001, a cosine learning rate schedule [39], and 3 training epochs. In the expert projections training, the learning rate starts at 0.0625 and decays to 0.056 after 3 epochs for LLaVA-1.5-7B [36], and starts at 0.1 and decays to 0.0904 after 3 epochs for LLaVA-NeXT-13B [35]. The MoE gating module training is the same for both LLaVA models, with the initial learning rate set to 0.2 and decaying to 0.1809 after 3 epochs.

An effective batch size of 8 is used across all settings: in the expert projections training for LLaVA-1.5-7B and for the gating module, a batch size of 2 with 4 gradient accumulation steps is used. In the expert projections training for LLaVA-NeXT-13B, a batch size of 1 with 8 gradient accumulation steps is used. Gradient checkpointing is applied during the expert projections training for LLaVA-NeXT-13B to reduce GPU memory usage.

CLIP-UP is designed to enhance UPD capabilities and is not intended to improve overall accuracy (*i.e.*, on standard answerable questions). For this reason, we filter the training data to include only questions that the original model can correctly answer (*e.g.*, for LLaVA-1.5-7B, the data include only multiple-choice VQA questions that the original LLaVA-1.5-7B answers correctly). Additionally, training is performed with the same order of samples in each epoch, which we found to improve training stability.

We generate the correlation vectors using Structure-CLIP [25]. Its embedding dimension is 768, resulting in a total dimension of 3072 for the four concatenated correlation vectors. Consequently, each expert linear projection layer contains 12.6M parameters for LLaVA-1.5-7B (with an intermediate feature space dimension of 4096) and 15.7M parameters for LLaVA-NeXT-13B (with an intermediate feature space dimension of 5120). The gating linear layer contains only 18K parameters (same for both models).

CLIP-UP training and inference are conducted using the base setting, *i.e.*, the model is provided with multiple-choice VQA inputs without additional instructions. All experiments are performed using greedy decoding.

LLaVA’s LLM component is quantized to 4 bits during training, while inference is performed without quantization. All the projection layers include bias terms and operate in bfloat16 precision. CLIP-UP training is conducted on a sin-

gle NVIDIA RTX A5000 GPU for LLaVA-1.5-7B, and on a single NVIDIA RTX A6000 GPU for LLaVA-NeXT-13B.

Structure-CLIP. As noted in Sec. 4.2, we fine-tune Structure-CLIP ourselves [25]. Fine-tuning is performed on CLIP ViT-L/14@336px [47] for one epoch on a single NVIDIA A100 GPU, over the MS COCO dataset [33] with augmentations by [25]. To reduce memory usage, we freeze the first 9 transformer blocks of the image encoder and the first 21 transformer blocks of the text encoder. The Knowledge-Enhanced Encoder (KEE) component is fine-tuned following the procedure in [25]. We use a learning rate of 3×10^{-6} , a batch size of 16, a weight decay of 0.1, and a KEE Knowledge weight of 0.2. In inference we use the fine-tuned image and text encoders of Structure-CLIP without the additional KEE.

Full-model fine-tuning. In the main paper we compare CLIP-UP to full-model LoRA fine-tuning [23] on UPD data [42]. We use the LLaVA-NeXT-13B LoRA weights published by [42]. For LLaVA-1.5-7B, we perform the LoRA fine-tuning ourselves following the procedure described in [42], as this model was not tested in their work.

B. Evaluation details

UPD evaluation. We conducted all the UPD evaluations ourselves, including those of the prompt engineering methods. For all experiments that were also performed by Miyai et al. [42], our results closely align with theirs. For each CLIP-UP experiment, we trained with 3 different seeds (determining the order of samples) and selected the weights that achieved the best performance on the validation set.

UPD evaluation requires extracting the selected option from the model’s prediction. We followed the extraction approach described in [42]: each VLM prediction is first processed using a string matching algorithm, and if this fails, GPT-3.5 (gpt-3.5-turbo-0125 [44]) is employed with a tailored prompt to extract the selected option. We introduced slight modifications to the string matching algorithm to improve efficiency and accuracy, and reduce calls to GPT-3.5. To ensure fair comparison, all UPD results were evaluated using our modified string matching extraction algorithm.

Evaluation on other tasks. The evaluation of tasks beyond multiple-choice VQA was conducted using VLMEvalKit [13]. The following metrics were measured

(see Tab. 2): for MME [14], “Score” represents the overall perception and reasoning scores, “Acc.” denotes the percentage of correct answers, and “Y/N” denotes the percentage of responses identified as “yes” or “no”. MM-VET [58] is evaluated by its overall score. LLaVA-Bench (In-the-Wild) [36] score reflects the overall relative performance. Please refer to the sources for more details.

C. Dataset

We provide details about the dataset created for training CLIP-UP. The goal was to create a compact UPD training dataset. We do not use the fine-tuning dataset from [42] as it is too large (10,000 samples), lacks IASD samples, and, upon our manual inspection, found to be of insufficient quality.

The dataset is organized into multiple-choice VQA question pairs, each consisting of a standard answerable question and its corresponding unanswerable variant. The training set contains 263, 159, and 277 question pairs for AAD, IASD, and IVQD, respectively (a total of 526, 318, and 554 samples). The validation set contains 30 pairs for each category. We do not include a test set.

Unlike the training set, each question in the validation set is augmented to have n repetitions (n is the number of options), each with a different circular shift of the options. This allows the measurement of dual accuracy on the validation set. Consequently, the validation set contains a total of 204, 232, and 226 questions for AAD, IASD, and IVQD, respectively.

The dataset was created with a different process for each unanswerability category, as we explain below. All data were sourced from public training sets to ensure no overlap with the MMBENCH benchmark [38], from which the MM-UPD benchmark [42] was derived. For all categories, questions were generated with four options. Most questions were left unchanged, but some were modified to include fewer options. We also ensured that the correct option varies (*e.g.*, it is not always “A”).

Note that the dataset was constructed in a straightforward manner, resulting in uniform questions, as we assumed this would suffice for training CLIP-UP. This simplicity highlights CLIP-UP’s robustness and suggests that a more diverse dataset could further improve performance.

C.1. AAD data

The AAD data consist of 293 pairs of questions: 143 pairs sourced from the A-OKVQA dataset [50], and 150 pairs generated using GPT-4o mini [45] based on MS COCO [33].

Our goal is to have standard questions with exactly one correct answer option, while all others are clearly incorrect. This ensures that AAD unanswerable questions may be generated by removing the correct answer option, leaving no

valid answer in the answer options set. Note that this condition is not always met, as many questions are intentionally designed to be challenging, requiring the selection of the best option from several plausible ones.

We began by creating the standard questions, selecting 143 multiple-choice VQA questions from the A-OKVQA training dataset [50]. We manually examined the data and included only questions with exactly one correct answer option.

We created 150 additional standard questions using the following process: we first sampled examples from MS COCO training set [33] (2017 split). Each sample consists of an image and five ground truth captions, from which we randomly selected one. Next, we used GPT-4o mini [45] to generate three incorrect captions for each sample. GPT-4o mini was given an image and its correct caption, and instructed to output a multiple-choice VQA question asking to select the correct caption, with four answer options: a correct one (the ground truth caption) and three incorrect ones (generated by GPT-4o mini). See the instruction used in Fig. 5a. To diversify the data, we alternated between two question formats: “Which caption describes the image?” and “Which one is the correct caption for this image?”. As with the A-OKVQA questions, we included only standard questions with exactly one correct answer option.

After obtaining 293 standard multiple-choice VQA questions from both sources, we created the AAD counterparts by removing the correct answer option from each standard question. See Fig. 6a for an example.

C.2. IASD data

The IASD data consist of 189 pairs of questions. In the case of IASD, there are no specific constraints on the standard questions. However, for the unanswerable questions, the textual question (the question itself, *e.g.*, “What color is the dress?”) and the answer options set must be incompatible.

Similar to the AAD case, we used standard questions from the A-OKVQA training dataset [50] and ones generated with GPT-4o mini [45]. To create the unanswerable counterpart for each standard question, the original answer set was replaced with one from another randomly selected standard question. We then manually examined the data to include only pairs where the textual question is genuinely incompatible with the unanswerable answer options set. See Fig. 6b for an example.

C.3. IVQD data

The IVQD data consist of 307 pairs of questions: 42 pairs sourced from the fine-tuning data by [42], and 265 pairs generated using GPT-4o mini [45] based on MS COCO [33] and TextCaps [51].

Our goal is to have pairs of multiple-choice VQA questions where the textual question conveys some specific in-

formation about the image. This allows generating unanswerable IVQD questions by replacing the image with another image that is incompatible with the information in the textual question (in contrast, non-specific questions like “What emotion does this image convey?” are compatible with most images).

The 42 pairs sourced from the fine-tuning data by [42] include corresponding standard and IVQD unanswerable questions. We manually ensured that in all pairs, the textual question conveys image-specific information and is genuinely incompatible with the image in the unanswerable item.

For the 265 other question pairs, we generated standard questions using the following process: similar to the AAD case, we sampled examples from MS COCO training set [33] (2017 split), but also from TextCaps training set [51]. Each sample consists of an image and five ground truth captions, from which we randomly selected one. Next, we used GPT-4o mini [45] to generate an image-specific textual question from each caption. GPT-4o mini was given a caption (without the image) and instructed to output an image-specific textual question related to the caption along with the correct answer. See Fig. 5b for the instruction used. Then, we used GPT-4o mini to create three incorrect answer options for each question by providing it with the image, question and correct answer as input, and instructing it similarly to the AAD case.

To create the unanswerable counterpart for each standard question, we replaced the image with one from another randomly selected standard question. The data were manually reviewed to include only pairs where the textual question is image-specific and genuinely incompatible with unanswerable IVQD image. See Fig. 6c for an example.

D. Parsing question prompts

This section describes the rule-based algorithm mentioned in the main paper. The algorithm serves two purposes: first, to determine whether a textual input is a multiple-choice question. If it is, we generate the new embedding vector and integrate it into the VLM. Second, in case the input is a multiple-choice question, the algorithm parses it to separate the textual question and answer options, a step necessary for generating the new embedding vector (as explained in Sec. 3.2).

This algorithm relies on simple string matching and assumes a specific structure of multiple-choice question prompts: a question followed by answer options, each preceded by a letter (*e.g.*, “A”). For example, “What animal is by the flowers? A. Dog B. Rabbit C. Cat”.

In the first step, the algorithm determines whether the input is a multiple-choice question by checking for the presence of “A.” and “B.” (since a question must have at least two options). If these are present in the input, the algo-

rithm proceeds to the next step, where it parses the input: the question is the text before “A.”, the first answer option is the text between “A.” and “B.”, and so on for the remaining answer options.

Since the algorithm relies on string matching, it can be easily adjusted to support different input formats (*e.g.*, options denoted with numbers instead of letters). Moreover, it could be replaced with a more sophisticated approach, such as utilizing the LLM component of the VLM. We however found it unnecessary given the simplicity of the parsing task.

E. Additional results

Tab. 4 presents the complete results of our UPD experiments, including regular standard accuracy and regular UPD accuracy.

Fine-tuning using CLIP-UP training data. Tab. 4 also presents results of full-model fine-tuning [42] using CLIP-UP’s training data. Fine-tuning was conducted under the same settings as the original fine-tuning but with 3 epochs instead of one, for a fair comparison with CLIP-UP.

The results indicate that this fine-tuning setting achieves reasonable performance, but is inferior to both original fine-tuning and CLIP-UP. Notably, this setting involves significantly less data than the original fine-tuning setting (1,330 samples compared to 10,000 samples).

Training and inference times. We report the training and inference times for CLIP-UP. On LLaVA-1.5-7B, the expert projections training times for AAD, IASD, and IVQD are 13.4, 7.9, and 14.6 minutes, respectively. On LLaVA-NeXT-13B, the training times for AAD, IASD, and IVQD are 90.4, 53.0, and 98.3 minutes, respectively. The MoE gating module training time is 2 minutes. We note that LLaVA-NeXT-13B is slow due to its high image resolution, in addition to our use of gradient checkpointing during training.

CLIP-UP has a marginal impact on inference time, as the new embedding vector is generated only once per input and is cached for reuse. On the IVQD sub-benchmark from MM-UPD, inference by LLaVA-1.5-7B with CLIP-UP takes 16.22 minutes, compared to 18.07 minutes with the base setting. Per-token inference time shows a 16% increase with CLIP-UP compared to the base setting (0.04665 seconds per token versus 0.04028 seconds per token).

Method	AAD					IASD					IVQD					Dual Avg.
	Reg. Stand.	Circ Stand.	Reg. UPD.	Circ. UPD.	Circ. Dual	Reg. Stand.	Circ Stand.	Reg. UPD.	Circ. UPD.	Circ. Dual	Reg. Stand.	Circ Stand.	Reg. UPD.	Circ. UPD.	Circ. Dual	
Original Model	79.07	70.73	0.04	0.00	0.00	76.91	68.12	0.37	0.33	0.33	73.80	65.45	0.00	0.00	0.00	0.11
Base Setting	77.56	69.15	3.69	1.46	1.46	75.67	66.81	28.47	19.48	12.73	72.59	63.76	0.68	0.28	0.28	4.82
Addit.-Option*	75.93	68.29	55.87	48.66	40.85	73.94	65.61	85.42	78.02	51.03	73.49	64.33	37.73	27.81	22.19	38.02
Addit.-Instruction*	75.96	69.02	41.20	33.90	28.05	74.02	66.16	77.99	65.72	43.74	72.97	64.61	42.77	32.02	24.44	32.08
CLIP-UP-Expert*	72.37	62.44	94.07	90.73	58.41	71.98	62.68	93.65	88.14	55.71	71.61	62.92	92.32	87.64	55.34	56.49
Fine-tun. [†]	73.35	64.63	66.00	56.34	43.78	71.04	61.92	93.02	87.81	54.73	69.28	61.24	92.77	85.96	52.25	50.25
Fine-tun. (CU data) [†]	73.41	66.71	60.66	51.10	40.49	70.93	63.33	93.17	88.25	55.71	69.05	61.80	78.61	67.70	44.66	46.95
CLIP-UP (ours)	69.63	59.39	81.52	77.07	48.54	67.78	57.45	92.12	89.12	52.34	67.02	57.58	92.47	88.20	53.09	51.32

(a) LLaVA-1.5-7B

Method	AAD					IASD					IVQD					Dual Avg.
	Reg. Stand.	Circ Stand.	Reg. UPD.	Circ. UPD.	Circ. Dual	Reg. Stand.	Circ Stand.	Reg. UPD.	Circ. UPD.	Circ. Dual	Reg. Stand.	Circ Stand.	Reg. UPD.	Circ. UPD.	Circ. Dual	
Original Model	83.86	76.71	0.00	0.00	0.00	80.80	73.23	0.20	0.11	0.00	79.97	71.35	0.00	0.00	0.00	0.00
Base Setting	81.53	72.32	34.00	23.78	17.80	79.18	69.75	62.76	49.62	31.66	77.86	68.82	56.78	44.66	33.15	27.54
Addit.-Option*	83.10	75.85	23.36	18.41	18.05	80.03	72.47	55.02	39.28	29.92	79.37	70.79	53.54	46.35	38.20	28.72
Addit.-Instruction*	77.12	67.07	60.28	48.66	38.29	73.91	63.87	93.53	87.81	57.02	78.31	68.82	79.59	71.91	54.49	49.93
CLIP-UP-Experts*	78.89	70.37	87.11	81.22	60.24	73.68	64.09	96.28	93.14	59.96	77.48	67.42	95.11	93.82	65.17	61.79
Chain-of-Thought	–	60.00	–	60.50	42.80	–	56.40	–	70.80	43.90	–	59.00	–	75.30	47.50	44.73
Self-Reflection	–	66.20	–	50.00	37.80	–	62.60	–	55.80	36.70	–	59.80	–	61.50	39.00	37.83
Fine-tun. [†]	78.35	69.15	65.41	58.54	47.56	75.33	65.51	94.84	91.19	59.85	76.66	67.42	91.87	86.24	59.55	55.65
Fine-tun. (CU data) [†]	77.25	67.56	62.78	55.00	43.29	74.42	64.31	96.80	94.02	60.17	76.28	65.73	90.36	84.27	57.02	53.49
CLIP-UP (ours)	77.72	68.17	75.96	69.76	52.56	74.33	64.20	89.96	84.33	55.39	73.64	60.67	91.19	89.04	56.18	54.71

(b) LLaVA-NeXT-13B

Table 4. CLIP-UP full results (%) on the MM-UPD benchmark [42] for (a) LLaVA-1.5-7B and (b) LLaVA-NeXT-13B. Metrics include regular standard, regular UPD, circular standard, circular UPD, and circular dual accuracies. The best-performing methods that do not assume unavailable knowledge of unanswerability categories are bolded. “Fine-tun.” stands for full-model fine-tuning as done in [42]. “Fine-tun. (CU data)” stands for full-model fine-tuning with CLIP-UP training data. *Methods assuming knowledge of unanswerability categories. [†]Fine-tuning degrades performance on other tasks, making it an impractical solution.

You are an assistant with the task of creating multiple-choice questions about images. You will be given an image, and its correct caption. The correct caption is the correct answer to the question “Which one is the correct caption of this image?”.

Your job is to create 3 distractors that are incorrect captions for the image. Note that the distractors must be incorrect. This means that if we will take off the correct option, there will be no correct distractor that might describe the image. The output should be in the form of a python dictionary, with 6 entries: "question" containing the question, "image_id" containing an image id as integer (that will be given as input), "A" containing the correct caption, and "B", "C", "D" containing (each) the 3 distractors.

Here is an output for example: {"question": "Which one is the correct caption of this image?", "image_id": 57703, "A": "A man and two women walking their dogs and hiking in the woods.", "B": "A group of people camping near a lake with their pets.", "C": "Three hikers climbing a mountain trail with no animals in sight.", "D": "Two women and a child having a picnic in a grassy field."}

(a)

You are an assistant with the task of creating a “specific” question about an image. You will be given a caption of an image (without the image itself), and you should phrase a question that can be answered using the information in this caption. The question must be phrased so it delivers some information about the image, thus it will not be relevant for any image. In addition, the information in the caption must be necessary to answer the question. You may deliver only some information about the caption, and not all of it, use your judgment. Please try to output long answers when possible.

The output should be in the form of a python dictionary, with 3 entries: "image_id" containing an image id as integer (that will be given as input), "question" containing the question, and "answer" containing the answer.

For you to understand, here are some examples. Each example contains input and output, an additional undesired output with an explanation:

Example 1:

Input: {"image_id": 32677, "caption": "A dog and a cat sleeping next to each other."}

Output: {"image_id": 32677, "question": "What animals are sleeping in the image?", "answer": "A dog and a cat."}

Undesired output: {"image_id": 32677, "question": "What is in the image?", "answer": "A dog and a cat."}

Explanation: “What is in the image?” may be applied for any image, and thus it is an undesired question.

Example 2:

Input: {"image_id": 32678, "caption": "A yellow happy emoji."}

Output: {"image_id": 32678, "question": "What emotion does this emoji express?", "answer": "Happiness."}

Undesired output: {"image_id": 32678, "question": "What emotion does this image express?", "answer": "Happiness."}

Explanation: Mentioning a specific object, emoji, implies that there must be an emoji in the image. On the other end, “What emotion does this image express?” may be applied for any image (one may say any image conveys some emotion).

Example 3:

Input: {"image_id": 34512, "caption": "An image of the Empire State Building."}

Output: {"image_id": 34512, "question": "What is the name of the building in the image?", "answer": "The Empire State Building."}

Undesired output: {"image_id": 34512, "question": "What place is it in the image?", "answer": "The Empire State Building."}

Explanation: Mentioning a specific object, building, implies that there must be a building in the image. On the other end, “What place is it in the image?” may be applied for almost any image.


(b)

Figure 5. The instructions given to GPT-4o mini for (a) generating incorrect answer options for AAD multiple-choice questions and (b) generating image-specific questions for IVQD multiple-choice questions.

Standard

Question

Which caption describes the image?
 A. A blue train traveling through a mountainous landscape
 B. A cargo ship docked at a busy harbor with containers
 C. A black train parked next to a red train in a train station
 D. Two buses waiting at a city bus stop during rush hour




Correct Answer C. A black train parked next to a red train in a train station ✓

(a)

Unanswerable (AAD)

Question

Which caption describes the image?
 A. A blue train traveling through a mountainous landscape
 B. A cargo ship docked at a busy harbor with containers
 C. Two buses waiting at a city bus stop during rush hour




Correct Answer I cannot answer ✓

Standard

Question

What animals are these?
 A. Llama
 B. Donkey
 C. Horse




Correct Answer C. Horse ✓

(b)

Unanswerable (IASD)

Question

What animals are these?
 A. Fiction
 B. Biography
 C. Mathematics




Correct Answer I cannot answer ✓

Standard

Question

What type of vehicle is featured in the image?
 A. An antique pickup truck
 B. A bus
 C. A modern sports car
 D. A motorcycle




Correct Answer A. An antique pickup truck ✓

(c)

Unanswerable (IVQD)

Question

What type of vehicle is featured in the image?
 A. An antique pickup truck
 B. A bus
 C. A modern sports car
 D. A motorcycle



Correct Answer I cannot answer ✓

Figure 6. Pairs of standard and unanswerable multiple-choice VQA questions taken from our dataset for (a) AAD, (b) IASD, and (c) IVQD.